Cross talk between LAM cells and fibroblasts may influence alveolar epithelial cell behavior in Lymphangioleiomyomatosis

Clements D[1], Miller S[1], Babaei-Jadidi R[1], Adam M[4], Potter SS[4] and Johnson SR[1,2,3]

1. Translational Medical Sciences, University of Nottingham Biodiscovery Institute, Nottingham, UK
2. NIHR Biomedical Research Centre, University of Nottingham, Nottingham, UK
3. National Centre for Lymphangioleiomyomatosis, Nottingham University Hospitals NHS Trust, Nottingham, UK
4. Division of Developmental Biology, Cincinnati Children's Hospital Medical Center, Cincinnati, OH 45229, USA

Abstract

Lymphangioleiomyomatosis (LAM) is a female specific cystic lung disease in which *TSC2* deficient LAM cells, LAM-Associated Fibroblasts (LAFs) and other cell types infiltrate the lungs. LAM lesions can be associated with type II alveolar epithelial cells (AT2 cells). We hypothesized that the behavior of AT2 cells in LAM is influenced locally by LAFs. We tested this hypothesis in patient samples and *in vitro*.

In human LAM lung, nodular AT2 cells show enhanced proliferation when compared to parenchymal AT2 cells, demonstrated by increased Ki67 expression. Further, nodular AT2 cells express proteins associated with epithelial activation in other disease states including Matrix Metalloproteinase 7, and Fibroblast Growth Factor 7 (FGF7). *In vitro*, LAF conditioned medium is mitogenic and positively chemotactic for epithelial cells, increases the rate of epithelial repair and protects against apoptosis. *In vitro*, LAM patient-derived *TSC2* null cells cocultured with LAFs upregulate LAF expression of the epithelial chemokine and mitogen FGF7, a potential mediator of fibroblast-epithelial crosstalk, in an mTOR dependent manner. In a novel *in vitro* model of LAM, *ex vivo* cultured LAM lung-derived microtissues promote both epithelial migration and adhesion.

Our findings suggest that AT2 cells in LAM display a proliferative, activated phenotype and that fibroblast accumulation following LAM cell infiltration into the parenchyma contributes to this change in AT2 cell behavior. Fibroblast-derived FGF7 may contribute to the cross-talk between LAFs and hyperplastic epithelium *in vivo*, but does not appear to be the main driver of the effects of LAFs on epithelial cells *in vitro*.

Introduction

LAM is a rare, female predominant cystic lung disease in which cells of unknown origin infiltrate the lung parenchyma and the kidney to form distinctive lesions at these two sites (1, 2). In the lung, the presence of these cells is correlated with the formation of cysts and concomitant loss of lung function. The pulmonary lesions, or nodules, contain 'LAM cells', which harbour mutations in the tuberous sclerosis complex (TSC) tumour suppressor genes (3, 4), and other recruited cells including fibroblasts and immune cells (5-7). The growth of LAM nodules and the consequent destruction of the lung parenchyma is progressive, and ultimately can result in respiratory failure and death (8). Currently it is not clear how LAM nodules and cysts are associated, but it is assumed that unregulated protease activity results in destruction of collagen and elastin fibres that support parenchymal architecture (9-12).

Previously we showed that fibroblasts contribute to the community of cells within the LAM nodule (5); expression of Smooth Muscle Actin by LAM Associated Fibroblasts *in vivo* indicates that they are in an activated state, a phenotype associated with heightened proliferation and cytokine expression (9). Activated fibroblasts, in addition to providing a protective microenvironment for tumour cells, can contribute to disease outcome by pathogenic deposition of extracellular matrix (10-13) and recruitment other cells types into the tumour stroma (14).

Lung fibroblasts can exert a proliferative influence on type II alveolar epithelial (AT2) cells, and hyperplasia of type II pneumocytes has been identified as a characteristic of LAM although the signalling pathways involved remain poorly understood (15-19). Recent single cell studies of LAM lung tissue have also revealed transcriptional changes in alveolar epithelial cells consistent with an unusual activated phenotype (20, 21). We have isolated

LAM Associated Fibroblasts (LAFs) from a number of donors (5). We hypothesized that LAFs would stimulate AT2 cell proliferation and migration, and that AT2 cells around LAM nodules would display a proliferative phenotype. We tested these hypotheses using *in vitro* assays, including a novel *ex vivo* LAM microtissue assay, and LAM derived lung tissues to determine whether we could recapitulate the unusual behavior of AT2 cells in LAM.

Methods

Patient samples

Formalin-fixed paraffin-embedded (FFPE) LAM lung tissue blocks were collected from centres across the UK obtained from diagnostic biopsies, surgical procedures to treat pneumothorax or lung transplantation. Serum samples were obtained through the UK LAM Centre, Nottingham NHS Trust, where the patients were receiving clinical care. The study was approved by the East Midlands research ethics committee (Reference: 13/EM/0264). All subjects provided written informed consent and samples were used in accordance with the UK Human Tissue Act (2004).

Immunohistochemistry

Tissue for histological analysis was obtained from 32 individuals (26 diagnostic biopsies and 6 explanted lungs from transplantation for severe LAM) and whole histological sections stained with haematoxylin and eosin were re-reviewed by a pathologist to confirm a diagnosis of Lymphangioleiomyomatosis (LAM); this cohort is described in detail by Miller *et al* (22). Paraffin embedded LAM and control lung tissues were dewaxed in Histo-Clear II Histology Clearing Agent (SLS, Nottingham, UK) and rehydrated through an ethanol series (100%, 95%, 70%, water). If specified by the antibody supplier, antigen retrieval was carried out by heating sections to 100°C in a steamer for 15 minutes in 10 mM Sodium Citrate,

0.05% Tween 20, pH 6.0. Endogenous peroxidase activity was quenched by incubating sections in 3% H_2O_2 in water for 10 minutes at room temperature.

Primary antibodies used were: anti-Melanoma Associated Antigen PNL2 (1:50-1:100, Zytomed MSK082-05, RRID AB_2864524), mouse monoclonal anti-Smooth Muscle Actin (1:5000-1:10 000, Sigma Clone 1A4, A2547, RRID:AB_476701), mouse monoclonal anti-HOP (1:100, Santa Cruz Biotechnology Inc. sc-398703, RRID:AB_2687966), rabbit monoclonal anti-Prosurfactant Protein C antibody (1:1000, Abcam, ab90716, RRID:AB_10674024), mouse anti-Ki67 8D5 (1:500, Cell Signaling Technology, #9449, RRID:AB_2715512), rabbit polyclonal anti-KGF/FGF7 (1:2000, Abcam ab90259, RRID:AB_10714565), mouse monoclonal anti-MMP7 (ID2) (1:100, Chemicon Ab-3, RRID:AB_564871).

Secondary antibodies were AP or HRP conjugated goat anti-rabbit or anti-mouse (ImmPRESS Polymer Detection Kits, Vector Laboratories, MP-7451 and MP-7452) or Dako REAL EnVision detection system (Dako, K5007). Detection of primary antibodies was performed using ImmPACT DAB Peroxidase substrate (Vector Laboratories, SK-4105), ImmPACT AMEC Red Peroxidase Substrate (Vector Laboratories, SK-4285), or Vector Blue Alkaline Phosphatase Substrate (Vector Laboratories, SK-5300). Sections were counterstained with Mayer's haematoxylin, dehydrated through an ethanol series to Histo-Clear II Histology Clearing Agent (Scientific Laboratory Supplies Limited, NAT1334), and mounted in VectaMount Permanent Mounting Medium (Vector Laboratories, H-5000-60).

Isolation of 3D LAM lung microtissues

Where unpreserved viable LAM lung tissues were available within 24 hours of surgery, we used these to isolate small aggregates of cells which, on further analysis, proved to contain both LAM cells and fibroblasts. It seems likely that these are derived from un-disaggregated LAM nodules and we named them LAM microtissues by analogy with constructed 3D aggregates used as a model to elucidate tumour biology (23).

To generate LAM microtissues, LAM lung tissue was washed several times in serum-free Dulbecco's Modified Eagle's Medium – F12 without phenol red (DMEM/F-12, Thermo Fisher, 21041-033) containing penicillin, streptomycin and Amphotericin B (100 units penicillin, 0.1 mg streptomycin and 0.25 µg amphotericin B per mL, Sigma A5955), and then kept submerged at 4ºC overnight in this medium prior to further processing. Fragments of lung parenchyma free from pleura, major blood vessels and airways, approximately 0.5 cm^3-1 cm^3 were isolated and teased apart with fine forceps. Tissue was placed in collagenase solution (Sigma C6885 Collagenase from *Clostridium histolyticum*, 1mg/ml in serum free DMEM/F-12 medium, filter sterilised) and incubated at 37˚C for 2-4 hours with occasional agitation. Collagenase was inactivated by adding an equal volume of DMEM/F-12 with 10% Foetal Calf Serum (FCS). Cells were recovered by centrifugation (200*g*, 5 minutes) and resuspended in DMEM/F-12 + 10% FCS. After resuspension, cell clusters were allowed to sediment for 60 seconds. Suspended cells were removed and sedimented cell clusters were washed with fresh medium, and allowed to settle for 60 seconds before removing the medium. For inspection they were transferred to low attachment tissue culture plates (Corning Ultra-Low Attachment Dishes, Fisher Scientific).

Fluorescein diacetate viability assay on 3D LAM microtissues

Fluorescein diacetate (FDA, Sigma F7374) was prepared as a 5 mg/ml solution in water. This was diluted to a final concentration of 10 ug/ml in serum free, phenol red free DMEM/F-12. LAM microtissues were incubated in this staining medium for 5 minutes at room temperature then washed with fresh medium without serum before visualisation under epifluorescence on a Nikon Diaphot 300 inverted microscope using a FITC filter set.

Immunofluorescence

3D LAM microtissues were plated on 22 x 22 mm glass cover slips coated with collagen (PureCol Type I Bovine Collagen Solution, Advanced BioMatrix #5005) in six-well tissue culture plates and incubated for 3 days or until cells had extensively grown out. Cover slips were fixed for 10 min at room temperature with 4% formaldehyde, and permeabilized with 0.1% Triton X-100 in Phosphate Buffered Saline (PBS) for 5 min at room temperature. Samples were blocked with 2.5% normal goat serum (Vector Laboratories), then incubated with rabbit anti-gp100 (anti-Melanoma gp100 antibody [EP4863(2)], Abcam ab137078, RRID:AB_2732921) at 1:100 dilution overnight at 4 ˚C, followed by a fluorophore conjugated secondary antibody (Goat anti-Rabbit IgG (H+L) Cross-Adsorbed Secondary Antibody, Alexa Fluor 488, Thermo Fisher A-11008, RRID:AB_143165) for 1 hour at room temperature. After the final washes, cover slips were rinsed briefly in distilled water and then mounted in Fluorescence Mounting Medium (DakoCytomation S3023, Cambridgeshire, UK). Negative control was omission of the primary antibody.

Standard epifluorescence microscopy was performed using a Nikon Diaphot 300 inverted microscope, and images were captured using an Insight QE digital camera, with SPOT software (SPOT Advanced, RRID:SCR_016613, SPOT Imaging, Michigan, USA). Some fluorescent samples were captured as monochrome images for increased sensitivity.

LAM Associated Fibroblast culture

Primary LAM Associated Fibroblasts (LAFs) cells were cultured and characterised as described (5). Briefly, LAM lung tissue from diagnostic biopsy or diseased LAM lung removed at the time of lung transplantation was cut into small fragments, placed in collagenase solution (Sigma C6885 Collagenase from *Clostridium histolyticum*, 1 mg/ml in serum free DMEM/F-12, filter sterilised) and incubated at 37˚C for 2-4 hours with occasional agitation. Collagenase was inactivated by adding an equal volume of DMEM/F-12 with 10% FCS. Cells were recovered by centrifugation (200*g*, 5 minutes) and resuspended in DMEM/F-12 with 10% FCS, and the resulting suspension seeded into standard T75 tissue-culture flasks in medium comprising phenol red-free DMEM/F-12 supplemented with 10% FCS. Primary LAFs were characterised as described previously (5) and used at passage 3 to 6.

Proliferation assays

MTT reduction assays and direct cell counts pre- and post-exposure were used to measure cell proliferation. Experimental conditions were run in triplicate wells with at least three independent experiments performed. Where indicated the selective FGFR 1-3 inhibitor CH5183284/Debio-1347 (Selleck Chemicals Ltd., # S7665) was added at 100 nM in DMSO.

Boyden chamber migration assay

Boyden chamber migration assays were performed using 8.0 µm Transwell permeable supports (Costar #3422 6.5 mm tissue culture treated, polycarbonate) in 24 well plates. 100 µl serum-free DMEM/F-12 containing 1×10^5 A549 cells was added to the upper chamber and 600 µl serum free DMEM/F-12 or LAF conditioned DMEM/F-12 was added to the lower chamber. Plates were cultured at 37°C for 18 hours, then cells in each upper Transwell were

removed using a cotton swab, and cells on the bottom of the Transwell were fixed in 4% formaldehyde and stained with DAPI (4′,6-diamidino-2-phenylindole, Sigma D9542). Four fields of view were imaged per Transwell under epifluorescence on a Nikon Diaphot 300 inverted microscope, using a DAPI filter set, and migrated cells counted. All assays were performed in triplicate.

For migration assays involving LAM microtissues, A549 cells were labelled with CellTracker Green CMFDA Dye (Invitrogen, C2925) for 30 minutes, then were plated onto the underside of an inverted Transwell insert previously coated with collagen (PureCol Type I Bovine Collagen Solution, Advanced BioMatrix #5005). The insert was maintained in an inverted position for 2 hours then suspended in the well of a 24 well plate in serum free DMEM/F-12. LAM microtissues were introduced into the upper chamber in serum free DMEM/F-12 and the co-culture was maintained for 24 hours. Microtissues were imaged under epifluorescence on a Nikon Diaphot 300 inverted microscope, using a FITC filter set, to detect migrated A549 cells.

Scratch wound migration assay

A549 cells were plated at 50% confluence in a 24-well plate in DMEM/F-12 with 10% FCS, and allowed to grow to full confluence. A 200 µl pipette tip was used to generate a scratch wound across each well; the cells were then washed with serum-free medium to remove detached cells before adding 0.5 mls serum-free DMEM/F-12 medium or 0.5 mls LAF conditioned serum free DME-F12 medium. Wounds were imaged immediately and at the indicated time points on an Olympus CKX53 Inverted Microscope with a 4x objective using an Olympus XM10 digital camera and Olympus cellSens software (RRID:SCR_014551, Olympus Corporation).

Wound area was calculated in ImageJ (24) (RRID:SCR_003070, National Institutes of Health, Bethesda, MD, http://rsb.info.nih.gov/ij/), and the difference in wound area between the baseline and time points was used to determine the rate of wound healing. Four wounds were examined for each treatment.

Caspase 3/7 activity assay

A549 cells were plated at low density in 6 well plates and switched after 24 hours to either serum free DMEM/F12 medium or serum free DMEM/F12 medium conditioned for 24 hours by LAM associated fibroblasts (4 donors). After a further 24 hours incubation CellEvent Caspase 3/7 Detection Reagent (C10723, Invitrogen) was added to each well and cells were incubated for a further 30 minutes. Cells were fixed in 4% formaldehyde then stained with 1 µg/ml DAPI in PBS. Four fields of view were imaged per well under epifluorescence on a Nikon Diaphot 300 inverted microscope, using DAPI and FITC filter sets. Apoptotic cells with activated caspase-3/7 display green nuclei.

Microarray data analysis

Analysis of transcription changes in LAM associated fibroblasts from three donor when co-cultured with *TSC2* null 621-101 cells was described previously (25) (GEO datasets GSM4876064 - GSM4876069). The raw data were analysed using Transcriptome Analysis Console Software (Thermo Fisher, RRID:SCR_016519); genes which showed at least a 1.5-fold difference between monoculture and coculture conditions, with a p-value < 0.05, were considered statistically significant and differentially expressed.

cDNA Synthesis and Quantification of Gene Expression.

For quantitative real time RT-PCR total RNA was extracted from cells using RNeasy Mini Kit (Qiagen), contaminating genomic DNA removed using DNase I (Sigma, On-Column DNase I Digestion Set) and cDNA was synthesised using Superscript III First-Strand Synthesis System (Invitrogen) with random hexamer priming. Relative gene expression was determined by quantitative real-time PCR using pre-designed primers (KiCqStart SYBRGreen primers, Sigma) on a Stratagene Mx3005P thermocycler running MxPro software 9 RRID:SCR_016375). Reactions were performed in triplicate and expression levels of target genes determined relative to *β-actin* using the ΔCT method (26)**.**

FGF7 ELISAs

Quantification of FGF7 in cell culture supernatants was carried out using the Human KGF/FGF-7 DuoSet ELISA (R and D Systems, # DY251), while quantification of FGF7 in serum was carried out using the Human KGF/FGF-7 Quantikine ELISA (R and D Systems, # DKG00), according to manufacturer's instructions. Plates were read on a FlexStation 3 Multi-Detection Reader (Molecular Devices Corporation) and analysis carried out using SoftMaxPro software (Molecular Devices Corporation).

Single cell sequencing data analysis

Analysis of an existing LAM single cell sequence dataset was carried out (GEO GSE135851 (21)). Three LAM data sets were combined, and batch effects were minimized by using Seurat's canonical correlation analysis function, RunMultiCCA. Genes with the highest variability among cells were used for principal components analysis. Clustering was performed with Seurat's t-SNE implementation using significant principal components determined by JackStraw plot. Marker genes were determined for each cluster using Seurat's FindAllMarkers function using genes expressed in a minimum of 25% of cells and fold

change threshold of 1.3. Over/under clustering was verified via gene expression heatmaps. The cluster most enriched for SFTPC, representing type 2 alveolar epithelial cells, was subset and reclustered. SFTPB (for confirmation of identification) and FGF7 were plotted on the resulting reclustering to generate the feature-plots,

Statistical Analyses

Statistical analysis was performed using GraphPad Prism software version 9 (RRID:SCR_002798, GraphPad Software, Inc., La Jolla, CA). Paired experiments were analysed by t-test or Mann Whitney test, as indicated. Multiple comparisons were performed by Kruskal-Wallis test, (27), with Dunn's test of multiple comparisons (28) . P-values of <0.05 were regarded as significant.

Results

LAM lesions are associated with epithelial cell hyperplasia

LAM cells were identified in sections of paraffin embedded patient tissue from 34 women with LAM by reaction to both the anti-melanoma antibody PNL2 and to anti-Smooth Muscle Actin (Figure 1A, B). It was noted that in some samples LAM lesions were associated with accumulation of cells with a cuboidal epithelial morphology which did not react to PNL2 or anti-SMA; this feature was not uncommon, being noted to some degree in 6 out of 8 (75%) samples from patients who had undergone lung transplantation, and 12 out of 26 biopsy samples (46%). The cells were identified as Type 2 alveolar epithelial cells (AT2 cells) by reaction with anti-proSP-C, a highly specific marker of AT2 cells (29, 30) (Figure 1C). In areas of the samples with normal parenchyma, proSP-C expressing AT2 cells were dispersed along the alveolar walls (figure 1D).

Proliferating AT2 cells were identified in FFPE tissue from six LAM donors by dual immunohistochemistry for the nuclear proliferation marker Ki67 and for proSP-C (Figure 1E). In normal lung fewer than 1% of proSP-C expressing cells also expressed Ki67. Around LAM nodules, however, 4% of the nodular AT2 cells (+/- 1.4%) expressed both markers ($p = 0.0022$) (Figure 1F).

LAM associated nodular AT2 cells maintain SP-C expression and epithelioid morphology but are more proliferative than parenchymal AT2 cells. We sought to determine whether there were additional indicators of a dysregulated AT2 cell phenotype as noted by Obraztsova et al (20) in LAM, and seen in other diseases categorised by epithelial activation, such as idiopathic pulmonary fibrosis, where epithelial activation relates to disease activity (31). Consistent with an activated epithelial phenotype there was expression of the extracellular matrix protease Matrix Metalloproteinase 7 (MMP7) and the transcription factor HOP Homeobox (HOPX) in LAM associated nodular AT2 cells, which have previously been noted in activated or transitional phenotype AT2 cells in IPF (32, 33) and LAM (20). (Figure 1 G, H),

Modelling the LAM nodule: AT2 cell interaction *in vitro*.

The close association and prevalence of AT2 cells and LAM lesions could result from AT2 cell recruitment, increased proliferation or both. We sought to determine whether primary LAM associated fibroblasts could induce these processes in AT2 cells. In preliminary studies, primary AT2 cells did not maintain their phenotype, and lost proliferative and migratory properties *in vitro*; we therefore used the A549 human lung adenocarcinoma cell line (34) as

a model alveolar epithelial cell to determine whether we could recapitulate *in vitro* the behavior of AT2 cells seen *in vivo*.

Conditioned serum free medium from 3 separate LAF donors, harvested after 24 hours incubation (LAF CM) induced an increase in A549 cell number over 48 hours compared with serum free medium when assayed by cell counting, although this did not reach statistical significance ($p = 0.0641$, Figure 2A). Further, incubation with LAF conditioned medium was protective against apoptosis triggered by serum deprivation in A549 cells, when measured by an *in situ* caspase 3/7 activation assay. Incubation with LAF conditioned medium reduced the percentage of cells expressing active caspase 3/7 by 3.3% (+/- 0.67%) from 9.2% to 5.9% ($p = 0.0173$) (Figure 2B).

To determine if LAF conditioned medium was positively chemotactic for epithelial cells we used a Boyden chamber migration assay and a scratch wound healing assay. Compared with control media, LAF CM significantly increased both the rate of migration of A549 cells through a Transwell permeable membrane ($p = 0.0004$, Figure 2C) and the healing of a scratch wounded A549 monolayer ($p < 0.0001$, Figure 2D).

Epithelial cell migration in a novel *in vitro* 3D microtissue model

Previously we observed that LAFs are modified by exposure to LAM cells *in vitro* (25). It has not been possible to isolate and culture primary LAM cells from LAM lung tissue to determine whether LAFs exposed to LAM cells maintain the ability to stimulate epithelial cell migration. To circumvent this issue we created a novel assay system using three-dimensional (3D) LAM microtissues, i.e. aggregates of cells derived directly from LAM lung tissue using a limited collagenase digestion. LAM microtissues can be cultured on low

attachment culture surfaces, adopting a compact spherical morphology (Figure 3A, C). To determine the viability of LAM microtissues in culture we assayed fluorescein diacetate (FDA) uptake and cleavage; LAM microtissues were able to cleave FDA and retain the fluorescent product, showing they remain viable in culture over at least 7 days (Figure 3B, D)

In initial characterisation studies we confirmed that these structures contain fibroblasts and LAM cells by allowing the microtissues to adhere to tissue culture surfaces. Adhesion resulted in the emergence of fibroblasts with characteristic spindle morphology within 48 hours of adhesion (Figure 3 E, F). Additionally, a second cell population reacting to the anti-melanoma antibody anti-gp100 emerged over 4 days (Figure 3G, H).

When placed in the upper chamber of a migration chamber insert, LAM microtissues stimulated migration of A549 cells cultured on the underside of the chamber. The A549 cells, labelled with a fluorescent dye migrated upwards through the porous migration chamber membrane and adhered to the microtissues (Figure 3I, J). In the absence of LAM microtissues in the upper compartment, no upward migration of A549 cells was observed (not shown).

TSC2 null cells upregulate FGF7 expression in LAFs

We sought to identify soluble factors which could mediate the observed effects of LAFs on epithelial cells. Previously we examined how *TSC2* null LAM-derived cells affect the transcriptional profile of lung fibroblasts (25). In primary LAFs derived from human LAM lungs cultured with LAM-derived *TSC2* null 621-101 cells, we observed that transcription of *FGF7*, a known chemotactic and mitogenic factor for epithelial cells, was elevated in LAFs co cultured with 621-101 cells when compared with LAFs cultured alone (fold change = 1.9, $p = 0.0268$). The stimulation of *FGF7* transcription could be mediated by conditioned

359 medium from 621-101 cells. Treatment of 621-101 cells with rapamycin prior to collection of
360 conditioned medium significantly attenuated the upregulation of *FGF7* in LAFs (Figure 4A).
361 FGF7 secreted protein expression was also strongly upregulated in LAFs treated with 621-
362 101 conditioned medium, in a dose dependent manner (Figure 4B, $p = 0.0037$). Rapamycin
363 treatment of 621-101 cells prior to collection of conditioned media attenuated the increase in
364 transcription and secreted protein. 621-101 cells alone produced negligible amounts of FGF7
365 (Figure 4 C).
366
367 FGF7 is well established as a mitogen for epithelial cells (18, 35, 36). To determine whether
368 FGF7 signalling contributed to the mitogenic and chemotactic properties of LAF conditioned
369 medium towards epithelial cells we used DEBIO1347 a highly selective small molecule
370 fibroblast growth factor receptor (FGFR) 1, 2, 3 inhibitor (37) to attenuate these effects.
371 Whilst LAF conditioned medium increased A549 cell proliferation and migration, this was
372 not inhibited by treatment with DEBIO1347 (data not shown).
373
374 **FGF7 in LAM patient tissue**
375 Based on the stimulation of FGF7 expression in LAFs cocultured with 621-101 cells, we
376 hypothesized that LAFs in LAM lesions would express FGF7. We immunostained LAM lung
377 tissue from six women with LAM for FGF7 and noted FGF7 expression in spindle –shaped
378 cells within LAM lesions (Figure 5A). By double immunostaining with the anti-melanoma
379 antibody PNL2 we observed that FGF7 was expressed by nodule stromal cells that did not
380 react with PNL2 (Figure 5B). Since FGF7 is considered to be a growth factor produced by
381 mesenchymal cells we were surprised to note expression of FGF7 in LAM associated AT2
382 cells (Figure 5C), however to confirm this observation we analysed existing single cell
383 sequencing data from three patients with LAM (21), which revealed FGF7 expressing cells

384 within the cluster of lung cells expressing Surfactant protein C and Surfactant protein B
385 (Figure 5D).

386

387 **FGF7 as a serum biomarker in LAM**

388 To determine whether elevated levels of FGF7 in LAM lesions and associated alveolar
389 epithelial cells were reflected by higher serum levels of FGF7, we assayed FGF7 protein
390 levels by ELISA in serum samples from 22 healthy controls and 54 women with LAM. FGF7
391 was significantly elevated in serum of women with LAM relative to the controls ($p = 0.0297$).

392

393 **Discussion**

394 Previously we showed that the composition of LAM nodules is heterogeneous, and evolves as
395 lung disease worsens, with tuberin-deficient LAM cells becoming progressively outnumbered
396 by LAM-associated fibroblasts (22). Further, we determined that LAFs cocultured with
397 *TSC2*$^{-/-}$ LAM-derived cells underwent significant transcriptional changes, including
398 upregulation of inflammatory cytokines and other growth factors (25). Both Guo *et al.* (21)
399 and Obraztova *et al.* (20) recently noted transcriptional changes in LAM-associated AT2 cells
400 relative to cells derived from normal lung using single cell sequencing. Here we examined
401 whether the accumulation of modified fibroblasts in LAM could affect the properties of
402 neighbouring AT2 cells and hence impact disease progression.

403

404 In the normal lung AT2 cells are scattered through the parenchyma. They are relatively
405 quiescent, but proliferate slowly to give rise to both AT2 and AT1 cells (38). In LAM lung
406 tissue, nodules containing LAM cells and fibroblasts become associated with monolayers of
407 AT2 cells, identified by expression of the highly specific marker pro-Surfactant Protein C
408 (proSP-C), reflecting heightened recruitment or proliferation of nodular AT2 cells. This

effect was observed more frequently, although not significantly so in our available samples, in lung tissue derived from transplanted lungs than in tissue from biopsy or surgical procedures post pneumothorax and so may be a feature of late-stage disease. By immunohistochemistry we were able to demonstrate that AT2 cells associated with LAM lesions are markedly more proliferative than AT2 cells in undamaged areas of the parenchyma.

We sought to determine whether LAFs could promote epithelial cell migration or proliferation to account for the increased density of AT2 cells around LAM lesions. We found that LAF conditioned medium was both mitogenic and chemotactic for epithelial cells, and afforded protection against apoptosis induced by serum withdrawal. These observations suggest that the accumulation of LAFs associated with disease progression in LAM could contribute to the observed changed in AT2 cell distribution and proliferation.

LAM cells derived from diseased lung tissue cannot currently be grown in culture. We have developed a new *ex vivo* model which goes some way to addressing this issue. Microtissues derived from LAM lung tissue can be maintained in a viable state in culture and may recapitulate the features of the community of cells which constitute a LAM nodule. We are aware of the lack of availability of LAM lung tissue from which microtissues can be generated, but believe they have utility in enabling validation of results of *in vitro* experiments which have used model cell lines. In this model we were able to demonstrate recruitment and attachment of epithelial cells to LAM microtissues, reflecting the accumulation *in vivo* of epithelial cells around LAM nodules.

We also observed expression of MMP7 and HOPX in LAM-associated AT2 cells; MMP7 has previously been noted in activated epithelial cells in Idiopathic Pulmonary Fibrosis (IPF), a disease driven by abnormally activated fibroblasts (39) where serum MMP7 is also a predictive biomarker of disease progression (40). Homeodomain-Only Protein HOPX is generally expressed by AT1 cells in the healthy adult lung. Expression of HOPX by AT2 cells has been associated with loss of AT2 phenotype, including declining SP-C expression, and transdifferentiation to AT1 cells, often referred to as a 'transitional' phenotype. This is consistent with single cell sequencing data from LAM lung (20), which revealed an alveolar epithelial cell cluster with high expression of the AT2 markers *SFTPC* and *SFTPD*, and the AT1 marker *HOPX*.

Our previous analysis of primary LAM associated fibroblasts exposed *in vitro* to 621-101 $TSC2^{-/-}$ cells revealed numerous transcriptional changes (25). Here we identify elevated expression of the epithelial chemokine and mitogen FGF7 in LAFs exposed to 621-101 $TSC2^{-/-}$ cells, and observe expression of FGF7 in LAM lesions. Interestingly, Obraztsova *et al.* noted increased expression of FGF7 in *Tsc2*KO mouse lung mesenchyme (20), while *FGF7* is also expressed in the LAM^{CORE} cluster of cells identified by single cell analysis of LAM lung tissue (21).

We hypothesized that FGF7 might mediate crosstalk between LAFs and alveolar epithelial cells. In LAM patient tissue we showed that FGF7 is present in LAM nodule stroma and, unexpectedly, in associated AT2 cells. Serum FGF7 levels are higher in women with LAM than in healthy controls. However, blockade of FGFR signalling did not attenuate the ability of LAFs to stimulate epithelial cell proliferation or migration *in vitro*, indicating that other soluble factors are involved.

458

459 Distorted epithelial-mesenchymal cross-talk contributes to disease progression in Idiopathic
460 Pulmonary Fibrosis, where it is thought to result in enhanced fibroblast activation and
461 extracellular matrix synthesis. Whilst it remains to be seen whether parallels can be drawn
462 between pathogenic mechanisms in IPF and LAM, we have demonstrated that AT2 cells
463 associated with LAM lesions display a proliferative and transitional phenotype, and that
464 LAFs can potentially modify epithelial cell properties *in vivo.* Targeting this interaction may
465 provide new therapeutic options for LAM.

466

467 **Acknowledgements**

468 The authors thank the women with LAM who consented to participate in this research and
469 thank Professor Andrew Fisher (Freeman Hospital Newcastle, United Kingdom) for
470 facilitating access to LAM transplant tissue.

471

472 **Funding**

473 This work was supported by LAM Action [Program Grant] to SJ and the LAM Foundation
474 [LAM0108P01-15] to DC.

Bibliography

1. **Zhe X, and Schuger L**. Combined smooth muscle and melanocytic differentiation in lymphangioleiomyomatosis. *J Histochem Cytochem* 52: 1537-1542, 2004.
2. **Johnson SR, Taveira-DaSilva AM, and Moss J**. Lymphangioleiomyomatosis. *Clin Chest Med* 37: 389-403, 2016.
3. **Carsillo T, Astrinidis A, and Henske EP**. Mutations in the tuberous sclerosis complex gene TSC2 are a cause of sporadic pulmonary lymphangioleiomyomatosis. *Proc Natl Acad Sci U S A* 97: 6085-6090, 2000.
4. **Strizheva GD, Carsillo T, Kruger WD, Sullivan EJ, Ryu JH, and Henske EP**. The spectrum of mutations in TSC1 and TSC2 in women with tuberous sclerosis and lymphangiomyomatosis. *Am J Respir Crit Care Med* 163: 253-258, 2001.
5. **Clements D, Dongre A, Krymskaya VP, and Johnson SR**. Wild type mesenchymal cells contribute to the lung pathology of lymphangioleiomyomatosis. *PLoS One* 10: e0126025, 2015.
6. **Maisel K, Merrilees MJ, Atochina-Vasserman EN, Lian L, Obraztsova K, Rue R, Vasserman AN, Zuo N, Angel LF, Gow AJ, Kang I, Wight TN, Eruslanov E, Swartz MA, and Krymskaya VP**. Immune Checkpoint Ligand PD-L1 Is Upregulated in Pulmonary Lymphangioleiomyomatosis. *Am J Respir Cell Mol Biol* 59: 723-732, 2018.
7. **Osterburg AR, Nelson RL, Yaniv BZ, Foot R, Donica WR, Nashu MA, Liu H, Wikenheiser-Brokamp KA, Moss J, Gupta N, McCormack FX, and Borchers MT**. NK cell activating receptor ligand expression in lymphangioleiomyomatosis is associated with lung function decline. *JCI Insight* 1: e87270, 2016.
8. **Johnson SF, Davey DD, Cibull ML, Schwartz RW, and Strodel WE**. Lymphangioleiomyomatosis. *Am Surg* 59: 395-399, 1993.
9. **Peyser R, MacDonnell S, Gao Y, Cheng L, Kim Y, Kaplan T, Ruan Q, Wei Y, Ni M, Adler C, Zhang W, Devalaraja-Narashimha K, Grindley J, Halasz G, and Morton L**. Defining the Activated Fibroblast Population in Lung Fibrosis Using Single-Cell Sequencing. *Am J Respir Cell Mol Biol* 61: 74-85, 2019.
10. **Hoyles RK, Derrett-Smith EC, Khan K, Shiwen X, Howat SL, Wells AU, Abraham DJ, and Denton CP**. An essential role for resident fibroblasts in experimental lung fibrosis is defined by lineage-specific deletion of high-affinity type II transforming growth factor beta receptor. *Am J Respir Crit Care Med* 183: 249-261, 2011.
11. **Shoda H, Yokoyama A, Nishino R, Nakashima T, Ishikawa N, Haruta Y, Hattori N, Naka T, and Kohno N**. Overproduction of collagen and diminished SOCS1 expression are causally linked in fibroblasts from idiopathic pulmonary fibrosis. *Biochem Biophys Res Commun* 353: 1004-1010, 2007.
12. **Prasse A, Pechkovsky DV, Toews GB, Jungraithmayr W, Kollert F, Goldmann T, Vollmer E, Muller-Quernheim J, and Zissel G**. A vicious circle of alveolar macrophages and fibroblasts perpetuates pulmonary fibrosis via CCL18. *Am J Respir Crit Care Med* 173: 781-792, 2006.
13. **McDonald JA, Broekelmann TJ, Matheke ML, Crouch E, Koo M, and Kuhn C, 3rd**. A monoclonal antibody to the carboxyterminal domain of procollagen type I visualizes collagen-synthesizing fibroblasts. Detection of an altered fibroblast phenotype in lungs of patients with pulmonary fibrosis. *J Clin Invest* 78: 1237-1244, 1986.
14. **Qiu Z, Dillen C, Hu J, Verbeke H, Struyf S, Van Damme J, and Opdenakker G**. Interleukin-17 regulates chemokine and gelatinase B expression in fibroblasts to recruit both neutrophils and monocytes. *Immunobiology* 214: 835-842, 2009.
15. **Herrera I, Cisneros J, Maldonado M, Ramirez R, Ortiz-Quintero B, Anso E, Chandel NS, Selman M, and Pardo A**. Matrix metalloproteinase (MMP)-1 induces lung alveolar epithelial cell migration and proliferation, protects from apoptosis, and represses mitochondrial oxygen consumption. *J Biol Chem* 288: 25964-25975, 2013.
16. **Weng T, Poth JM, Karmouty-Quintana H, Garcia-Morales LJ, Melicoff E, Luo F, Chen NY, Evans CM, Bunge RR, Bruckner BA, Loebe M, Volcik KA, Eltzschig HK, and Blackburn MR**. Hypoxia-

induced deoxycytidine kinase contributes to epithelial proliferation in pulmonary fibrosis. *Am J Respir Crit Care Med* 190: 1402-1412, 2014.
17. **Konigshoff M, and Bonniaud P**. Live and let die: targeting alveolar epithelial cell proliferation in pulmonary fibrosis. *Am J Respir Crit Care Med* 190: 1339-1341, 2014.
18. **Panos RJ, Rubin JS, Csaky KG, Aaronson SA, and Mason RJ**. Keratinocyte growth factor and hepatocyte growth factor/scatter factor are heparin-binding growth factors for alveolar type II cells in fibroblast-conditioned medium. *J Clin Invest* 92: 969-977, 1993.
19. **Matsui K, W KR, Hilbert SL, Yu ZX, Takeda K, Travis WD, Moss J, and Ferrans VJ**. Hyperplasia of type II pneumocytes in pulmonary lymphangioleiomyomatosis. *Arch Pathol Lab Med* 124: 1642-1648, 2000.
20. **Obraztsova K, Basil MC, Rue R, Sivakumar A, Lin SM, Mukhitov AR, Gritsiuta AI, Evans JF, Kopp M, Katzen J, Robichaud A, Atochina-Vasserman EN, Li S, Carl J, Babu A, Morley MP, Cantu E, Beers MF, Frank DB, Morrisey EE, and Krymskaya VP**. mTORC1 activation in lung mesenchyme drives sex- and age-dependent pulmonary structure and function decline. *Nat Commun* 11: 5640, 2020.
21. **Guo M, Yu JJ, Perl AK, Wikenheiser-Brokamp KA, Riccetti M, Zhang EY, Sudha P, Adam M, Potter A, Kopras EJ, Giannikou K, Potter SS, Sherman S, Hammes SR, Kwiatkowski DJ, Whitsett JA, McCormack FX, and Xu Y**. Single-Cell Transcriptomic Analysis Identifies a Unique Pulmonary Lymphangioleiomyomatosis Cell. *Am J Respir Crit Care Med* 202: 1373-1387, 2020.
22. **Miller S, Stewart ID, Clements D, Soomro I, Babaei-Jadidi R, and Johnson SR**. Evolution of lung pathology in lymphangioleiomyomatosis: associations with disease course and treatment response. *J Pathol Clin Res* 6: 215-226, 2020.
23. **Napolitano AP, Dean DM, Man AJ, Youssef J, Ho DN, Rago AP, Lech MP, and Morgan JR**. Scaffold-free three-dimensional cell culture utilizing micromolded nonadhesive hydrogels. *Biotechniques* 43: 494, 496-500, 2007.
24. **Schneider CA, Rasband WS, and Eliceiri KW**. NIH Image to ImageJ: 25 years of image analysis. *Nat Methods* 9: 671-675, 2012.
25. **Babaei-Jadidi R, Dongre A, Miller S, Castellanos Uribe M, Stewart ID, Thompson ZM, Nateri AS, Bradding P, May ST, Clements D, and Johnson SR**. Mast-Cell Tryptase Release Contributes to Disease Progression in Lymphangioleiomyomatosis. *Am J Respir Crit Care Med* 204: 431-444, 2021.
26. **Livak KJ, and Schmittgen TD**. Analysis of relative gene expression data using real-time quantitative PCR and the 2(-Delta Delta C(T)) Method. *Methods* 25: 402-408, 2001.
27. **Kruskal WH, and Wallis WA**. Use of Ranks in One-Criterion Variance Analysis. *J Am Stat Assoc* 47: 583-621, 1952.
28. **Dunn OJ**. Multiple Comparisons Using Rank Sums. *Technometrics* 6: 241-&, 1964.
29. **Khoor A, Stahlman MT, Gray ME, and Whitsett JA**. Temporal-spatial distribution of SP-B and SP-C proteins and mRNAs in developing respiratory epithelium of human lung. *J Histochem Cytochem* 42: 1187-1199, 1994.
30. **Rooney SA, Young SL, and Mendelson CR**. Molecular and cellular processing of lung surfactant. *FASEB J* 8: 957-967, 1994.
31. **Tatler AL, and Jenkins G**. TGF-beta activation and lung fibrosis. *Proc Am Thorac Soc* 9: 130-136, 2012.
32. **Ota C, Ng-Blichfeldt JP, Korfei M, Alsafadi HN, Lehmann M, Skronska-Wasek W, M MDS, Guenther A, Wagner DE, and Konigshoff M**. Dynamic expression of HOPX in alveolar epithelial cells reflects injury and repair during the progression of pulmonary fibrosis. *Sci Rep* 8: 12983, 2018.
33. **Konishi K, Gibson KF, Lindell KO, Richards TJ, Zhang Y, Dhir R, Bisceglia M, Gilbert S, Yousem SA, Song JW, Kim DS, and Kaminski N**. Gene expression profiles of acute exacerbations of idiopathic pulmonary fibrosis. *Am J Respir Crit Care Med* 180: 167-175, 2009.
34. **Foster KA, Oster CG, Mayer MM, Avery ML, and Audus KL**. Characterization of the A549 cell line as a type II pulmonary epithelial cell model for drug metabolism. *Exp Cell Res* 243: 359-366, 1998.

35. **Rubin JS, Bottaro DP, Chedid M, Miki T, Ron D, Cunha GR, and Finch PW**. Keratinocyte growth factor as a cytokine that mediates mesenchymal-epithelial interaction. *EXS* 74: 191-214, 1995.
36. **Finch PW, Rubin JS, Miki T, Ron D, and Aaronson SA**. Human KGF is FGF-related with properties of a paracrine effector of epithelial cell growth. *Science* 245: 752-755, 1989.
37. **Nakanishi Y, Akiyama N, Tsukaguchi T, Fujii T, Sakata K, Sase H, Isobe T, Morikami K, Shindoh H, Mio T, Ebiike H, Taka N, Aoki Y, and Ishii N**. The fibroblast growth factor receptor genetic status as a potential predictor of the sensitivity to CH5183284/Debio 1347, a novel selective FGFR inhibitor. *Mol Cancer Ther* 13: 2547-2558, 2014.
38. **Barkauskas CE, Cronce MJ, Rackley CR, Bowie EJ, Keene DR, Stripp BR, Randell SH, Noble PW, and Hogan BL**. Type 2 alveolar cells are stem cells in adult lung. *J Clin Invest* 123: 3025-3036, 2013.
39. **Fujishima S, Shiomi T, Yamashita S, Yogo Y, Nakano Y, Inoue T, Nakamura M, Tasaka S, Hasegawa N, Aikawa N, Ishizaka A, and Okada Y**. Production and activation of matrix metalloproteinase 7 (matrilysin 1) in the lungs of patients with idiopathic pulmonary fibrosis. *Arch Pathol Lab Med* 134: 1136-1142, 2010.
40. **Bauer Y, White ES, de Bernard S, Cornelisse P, Leconte I, Morganti A, Roux S, and Nayler O**. MMP-7 is a predictive biomarker of disease progression in patients with idiopathic pulmonary fibrosis. *ERJ Open Res* 3: 2017.

Figure legends

Figure 1. LAM lesions are identified by immunoreactivity to both the anti-melanoma antibody PNL2 (A) and to anti-Smooth Muscle Actin (SMA) (B). The distribution of epithelial cells in the vicinity of LAM lesions is revealed by immunohistochemistry. (C) LAM lesions with PNL2 immunoreactivity (brown) are associated with epithelial cells, identified as Type 2 alveolar epithelial cells (AT2 cells) by expression of pro-surfactant C (blue) (D) Pro-surfactant C expression in AT2 cells in normal lung detected by immunohistochemistry. (E) Triple immunostaining of LAM lung sections with anti-Ki67 (brown, nuclear, arrowed), anti-proSP-C (blue) and anti-Smooth Muscle Actin (red-brown) demonstrates AT2 cells around LAM lesions are proliferative. (F) AT2 cells around LAM lesions are significantly more proliferative than AT2 cells in normal regions of parenchyma (Mann-Whitney test, $p = 0.0022$); a total of twelve hundred LAM nodule-associated and parenchymal proSP-C positive cells across six tissue donors were scored for Ki67 expression. AT2 cells around LAM nodules express MMP7 (G) and HOPX (H). Scale bar = 100μm unless otherwise indicated.

Figure 2. LAFs generate soluble factors which affect epithelial cell behavior**.**

(A) Serum free medium conditioned by 24 hours incubation with LAFs (LAF CM, four donors), shows mitogenic activity towards A549 cells when compared with serum free medium, assayed by cell counts after 48 hours treatment (Kruskal-Wallis test with Dunn's correction for multiple comparisons, $p= 0.0641$). 5% FCS = 5% foetal calf serum.

(B) A549 cells cultured in serum free medium display an increased rate of apoptosis compared with cells grown in medium containing 1% foetal calf serum. A549 cells grown in serum free medium conditioned by LAFs for 24 hours (LAF CM, three donors) have a

reduced level of apoptosis, measured by in situ Caspase 3/7 activity assay after 48 hours' incubation (Kruskal-Wallis test with Dunn's correction for multiple comparisons, $p = 0.0173$ for LAF CM vs serum free medium, $p = 0.0004$ for 1% foetal calf serum vs serum free medium).

(C) In a Boyden chamber migration assay, LAF conditioned medium (LAF CM, four donors) is positively chemotactic for A549 cells when compared with serum free medium. Migrated A549 cells on the underside of the porous migration chamber membrane were stained with DAPI and counted after 18 hours' incubation (Mann-Whitney test, $p = 0.0004$).

(D) LAF conditioned medium significantly increases the rate of healing of a scratch-wounded A549 monolayer. Following application of the scratch wound cells were incubated in serum free medium (Untreated), or LAF conditioned serum free medium (LAF CM, four donors). Four wounds were analysed per treatment. Wound area was measured immediately after wounding and after 48 hours (Mann-Whitney test, $p = <0.0001$).

Figure 3 A novel 3D cell culture system generated from patient samples recapitulates *in vivo* epithelial cell behavior.

LAM microtissues are isolated from LAM lung tissue by collagenase digestion followed by culture on non-adhesive plates (A, brightfield) and are viable after 24 hours culture, indicated by cleavage and retention of fluorescein diacetate (B, epifluorescence). After 7 days culture microspheres adopt a compact spherical morphology (C, brightfield) and retain viability (D, epifluorescence). On transfer to standard adhesive tissue culture treated plates fibroblast-like cells emerge after 24 hours (E, F). After 72 hours microtissues have fully dispersed (brightfield, G) and gp100-expressing cells can be detected by immunofluorescence. (H). In a Boyden chamber migration assay LAM microtissues promote migration and adhesion of

A549 epithelial cells. A549 cells labelled with CellTracker Green CMFDA (I, brightfield, J, epifluorescence). Scale bar = 250 μm.

Figure 4. Serum free medium was conditioned for 24 hours by 621-101 cells, or 621-101 cells treated for 24 hours with 10 nM rapamycin prior to growth in serum free medium. (A) LAFs grown in 621-101 CM (conditioned medium) for 4 days showed significant upregulation of *FGF7.* Treatment of 621-101 cells with 10nM rapamycin (621-101 + Rap) abolished this effect. (Mann-Whitney test with Dunn's multiple comparisons test, $p = 0.0037$ for serum free medium vs 621-101 CM, $p = 0.7159$ for serum free medium vs. 621-101 + Rap CM). Data pooled from four LAF donors.

(B) 621-101 CM also significantly increased FGF7 secreted protein expression, measured by ELISA, in a dose dependent manner. CM was diluted 1:8 (1:0.125x), 1:4 (0.25x), or 1:2 (0.5x) with serum free medium and LAFs incubated in this medium, or in serum free medium, for 72h. (Mann-Whitney test with Dunn's multiple comparisons test, $p = >0.9999$ for 1:8 dilution compared with serum free medium, $p = 0.0286$ for 1:4 dilution, $p = <0.0001$ for 1:2 dilution and undiluted). Data pooled from four LAF donors.

(C) Treatment of 621-101 cells with 10 nM rapamycin, with a subsequent wash-out, prior to collection of conditioned media attenuated the increase in secreted protein. 621-101 cells produce very low levels of FGF7. (Mann-Whitney test with Dunn's multiple comparisons test, $p = <0.0001$ for serum free medium vs. 621-101 CM, $p = 0.0110$ for serum free medium vs. 621-101+ Rap CM, $p = 0.1603$ for 621-101 CM vs. 621-101+ Rap CM). Data pooled from four LAF donors.

Figure 5. FGF7 can be detected in LAM lung lesions by immunohistochemistry (A, brown). Scale bar = 50 μm. Dual staining with anti-FGF7 (brown) and the anti-melanoma and LAM cell antibody PNL2 (blue) reveals expression in different cells. Scale bar = 100 μm (B). FGF7 expression was noted in nodular AT2 cells (brown, red arrow, C) in addition to nodular stromal cells (brown, black arrow). Scale bar = 200 μm. Panel D shows a t-distributed stochastic neighbour embedding (tSNE) plot of LAM lung cells, subset by expression of the Type 2 alveolar epithelial cell marker *SFPTC* (*Surfactant protein C*). All the cells express the type 2 alveolar epithelial cell marker *SFPTB* (*Surfactant protein B*), and a proportion of the cells also express *FGF7*. Gene expression is indicated by a blue overlay.

Figure 6. FGF7 levels in serum samples from 54 patients with LAM and from 22 healthy controls were measured by ELISA. Mean serum FGF7 concentration was significantly higher in LAM patients (t test, 8.91 pg/ml +/- 5.76 pg/ml) than in healthy controls (6.00 pg/ml +/- 3.31 pg/ml, p = 0.0297).

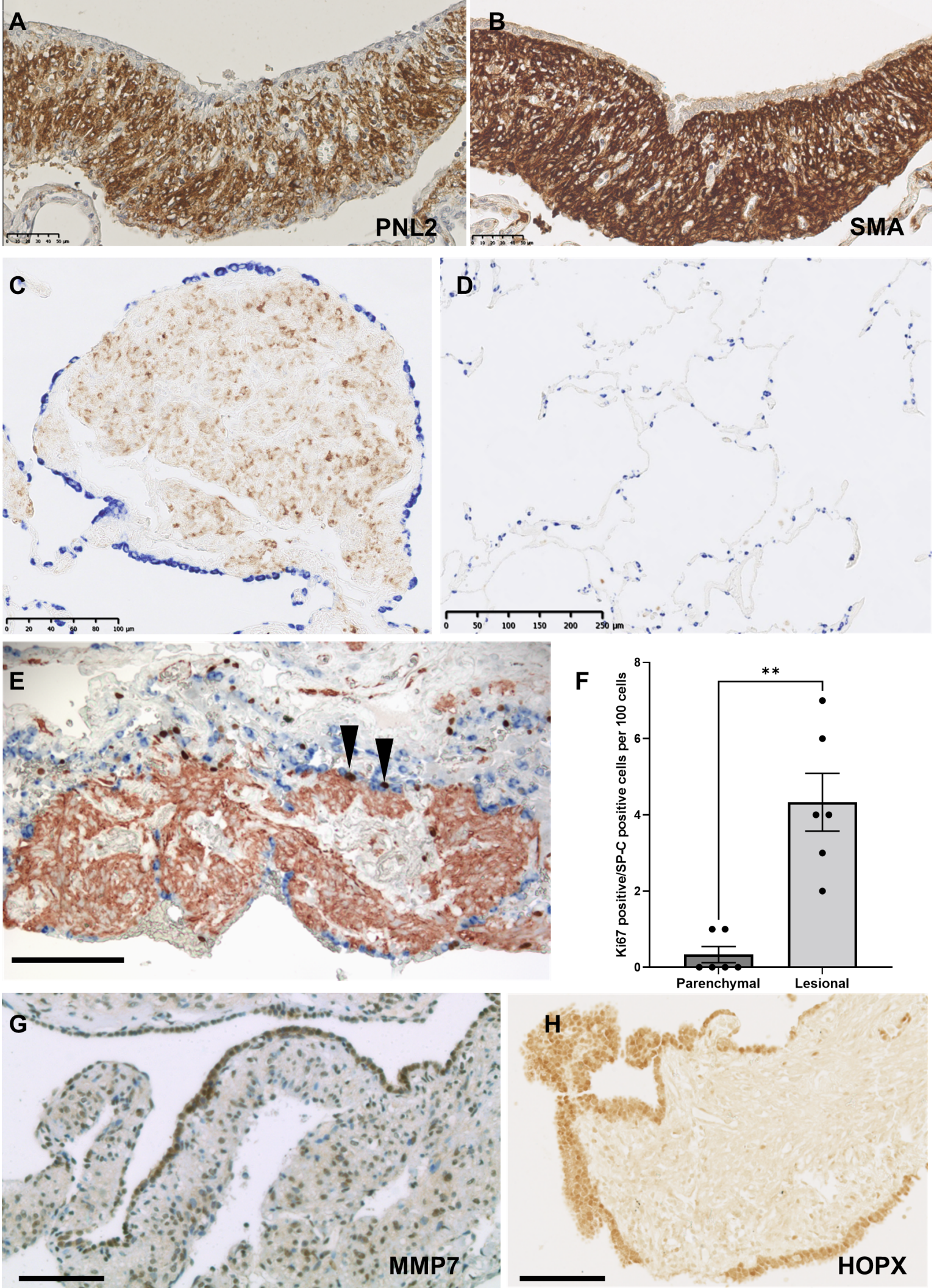
A
PNL2
B
SMA
C
0 20 40 60 80 100 µm
D
0 50 100 150 200 250 µm
E
F
Ki67 positive/SP-C positive cells per 100 cells
0
2
4
6
8
**
Parenchymal
Lesional
G
MMP7
H
HOPX

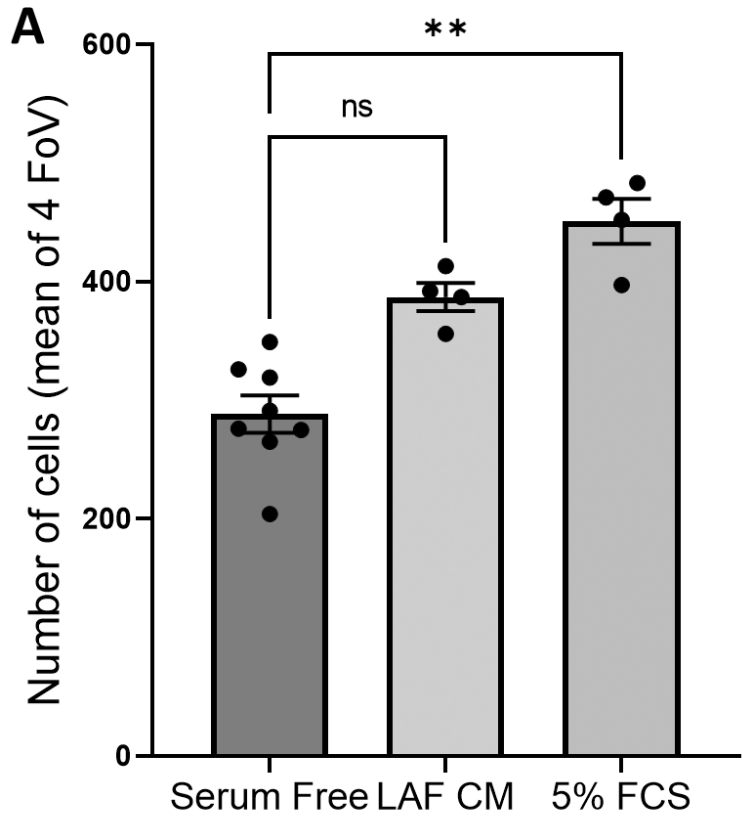
A
600
400
200
0
Number of cells (mean of 4 FoV)
**
ns
Serum Free
LAF CM
5% FCS

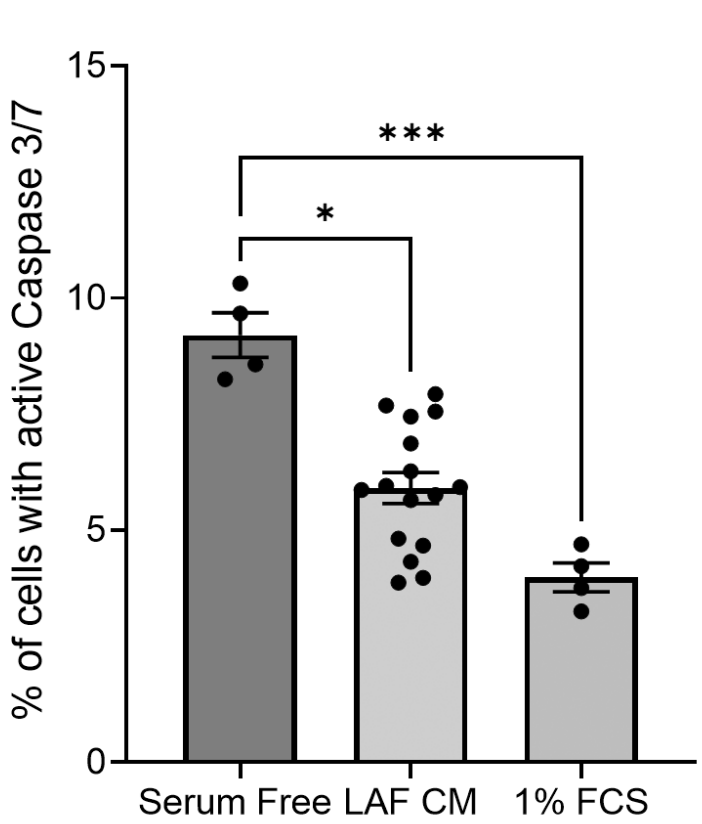
B
15
10
5
0
% of cells with active Caspase 3/7
***
*
Serum Free
LAF CM
1% FCS

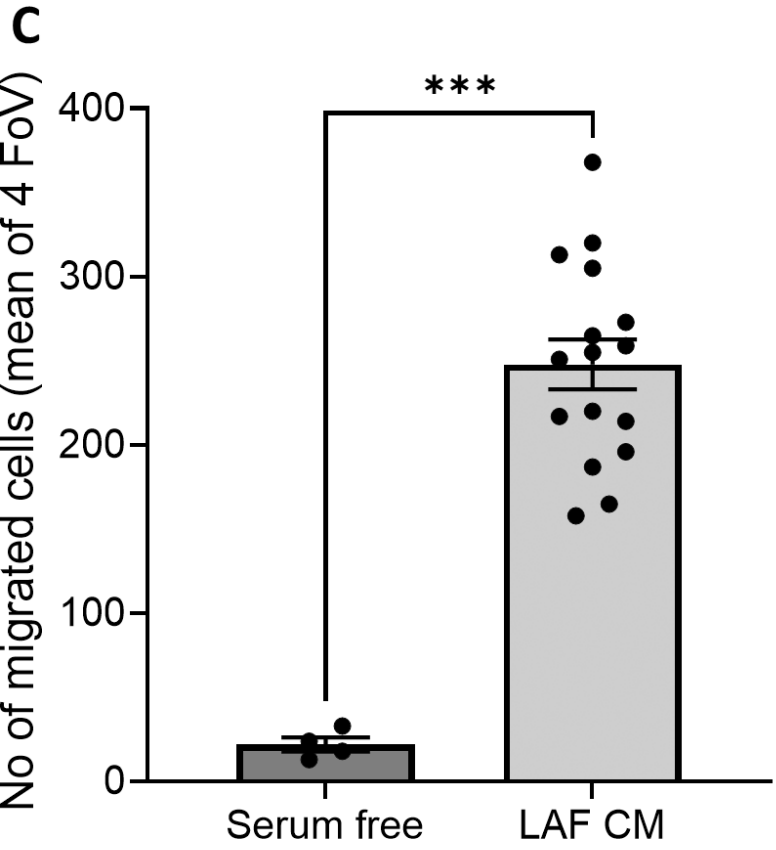
C
400
300
200
100
0
No of migrated cells (mean of 4 FoV)
***
Serum free
LAF CM

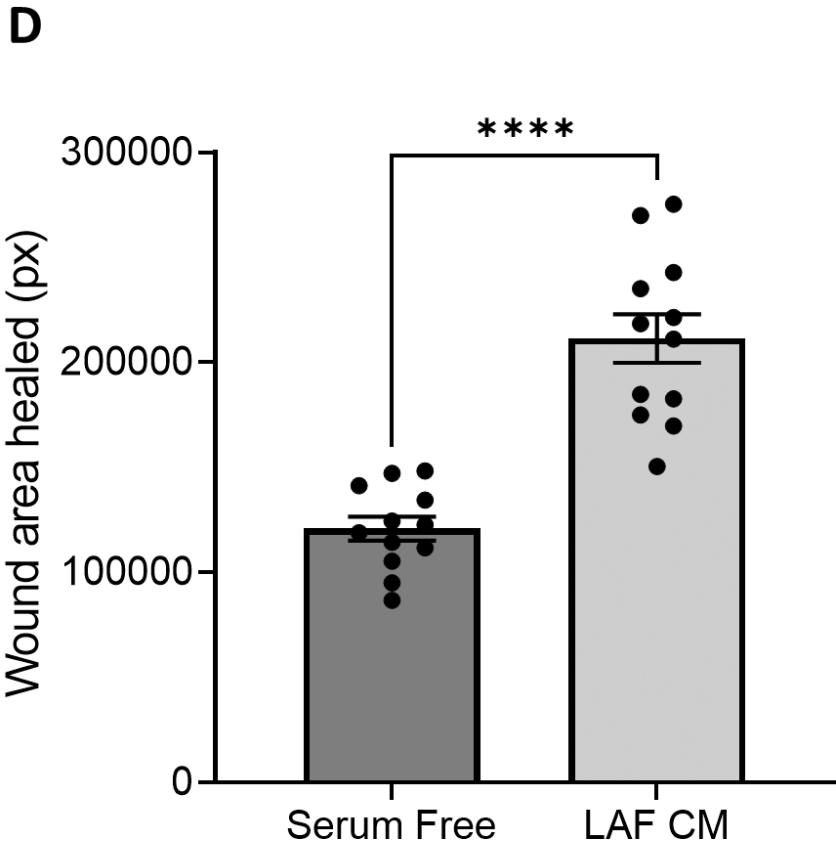
D
300000
200000
100000
0
Wound area healed (px)
****
Serum Free
LAF CM

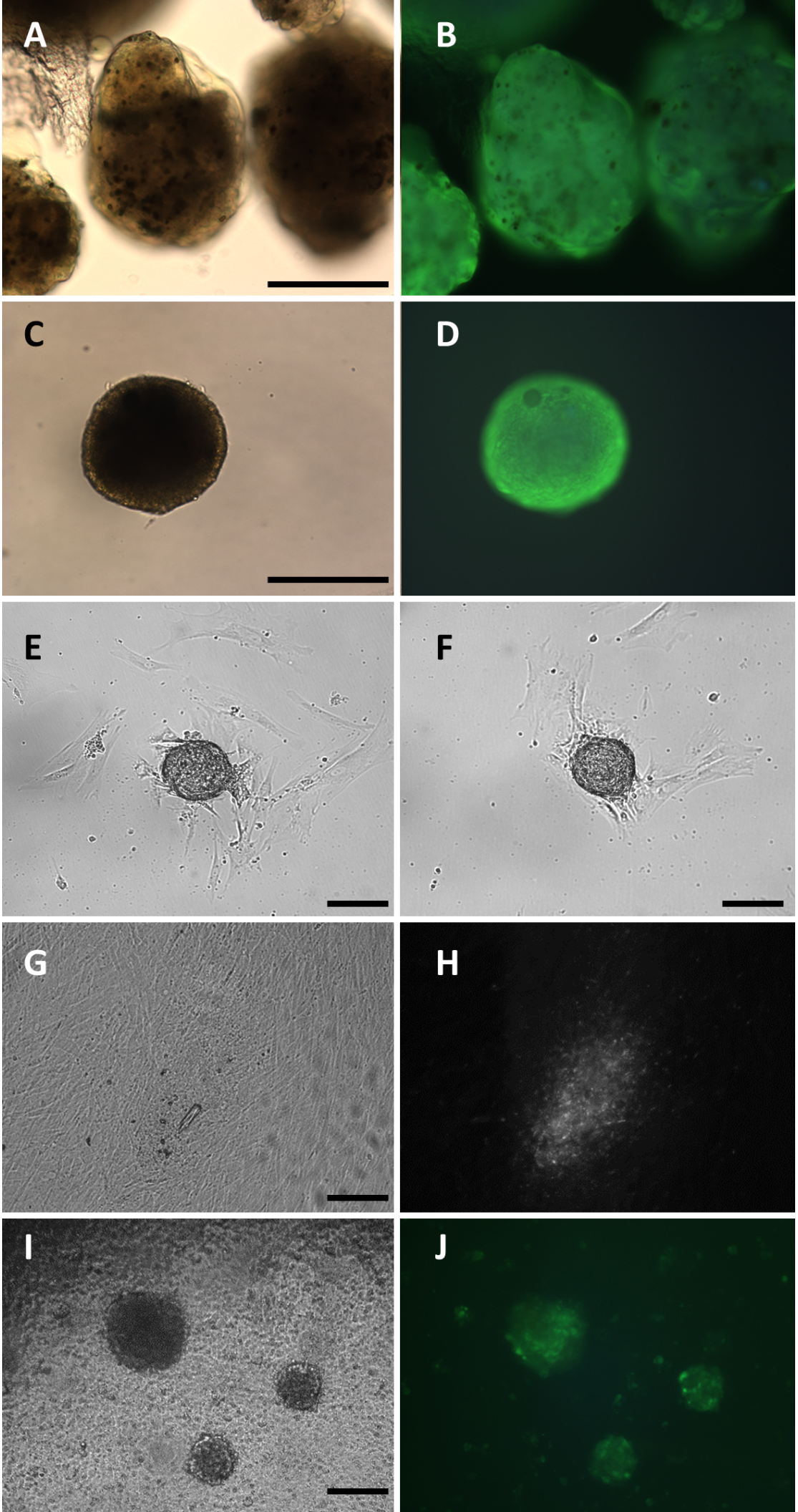
A
B
C
D
E
F
G
H
I
J

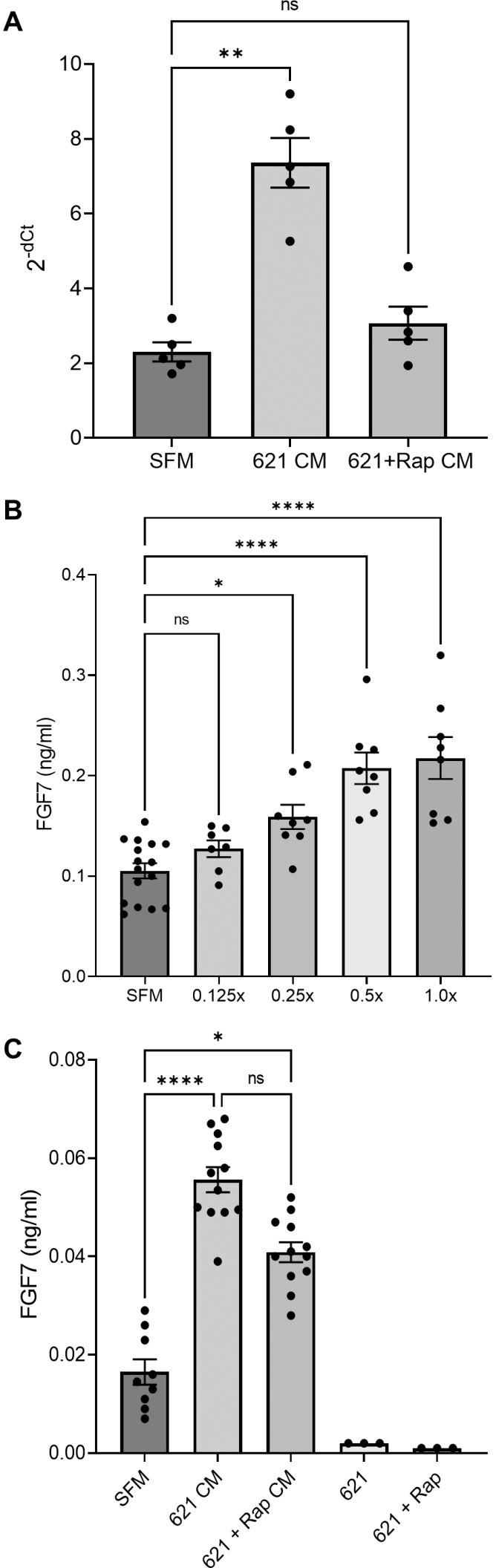
A
ns
**
10
8
6
4
2
0
2-dCt
SFM
621 CM
621+Rap CM
B
****
****
*
ns
0.4
0.3
0.2
0.1
0.0
FGF7 (ng/ml)
SFM
0.125x
0.25x
0.5x
1.0x
C
*
****
ns
0.08
0.06
0.04
0.02
0.00
FGF7 (ng/ml)
SFM
621 CM
621 + Rap CM
621
621 + Rap

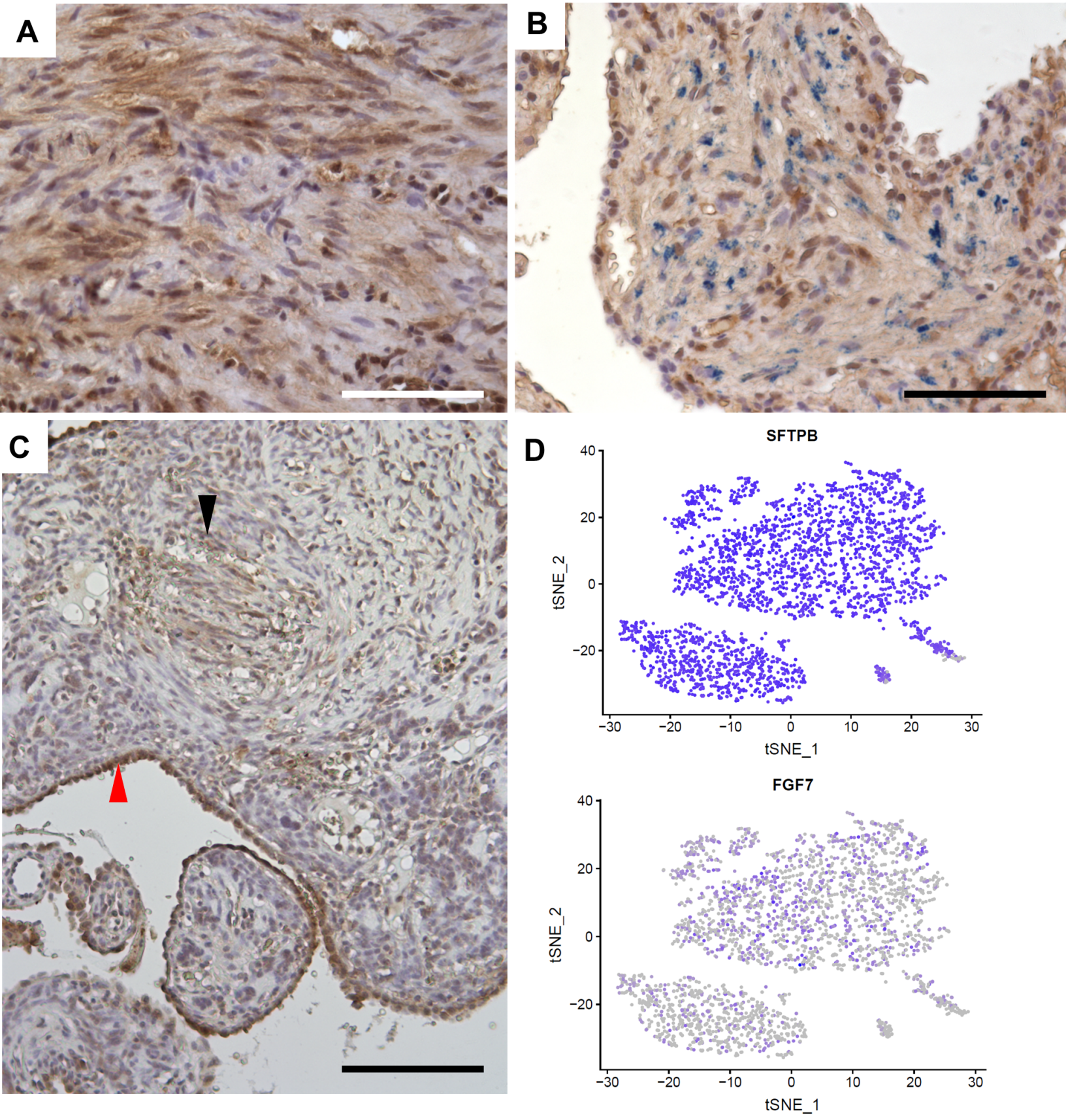
A
B
C
D
SFTPB
FGF7
tSNE_1
tSNE_2
40
20
0
−20
−30
−20
−10
0
10
20
30

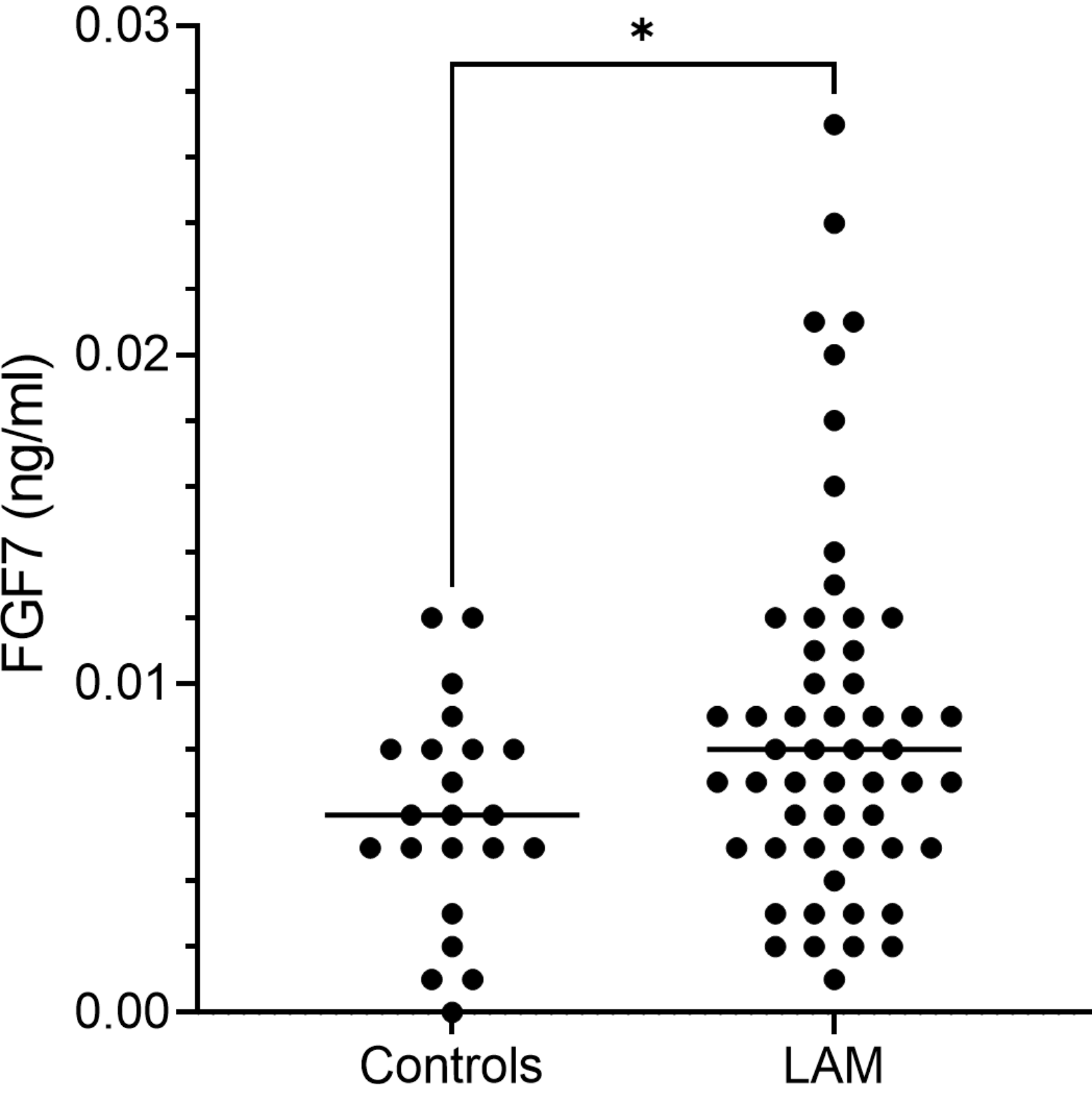
0.03
0.02
0.01
0.00
FGF7 (ng/ml)
*
Controls
LAM